Phys. Status Solidi B **250,** No. 2, 387–395 (2013) / **DOI** 10.1002/pssb.201248186

physica status solidi b
www.pss-b.com
basic solid state physics

# Anisotropic Curie temperature materials

**Jason N. Armstrong, Susan Z. Hua**, and Harsh Deep Chopra***

Laboratory for Quantum Devices, Mechanical and Aerospace Engineering Department, The State University of New York at Buffalo, Buffalo, NY 14260, USA

Received 22 March 2012, revised 3 October 2012, accepted 4 October 2012
Published online 29 October 2012

**Keywords** ac-calorimetry, anisotropic curie temperature, anisotropic magnetization, Arrott plots, heat capacity, spintronics

* Corresponding author: e-mail hchopra@buffalo.edu, Phone: +1 716 645 1415, Fax: +1 716 645 2883
** e-mail zhua@buffalo.edu, Phone: +1 716 645 1471, Fax: +1 716 645 2883

Existence of anisotropic Curie temperature materials [E. R. Callen, Phys. Rev. **124**, 1373 (1961); J. Appl. Phys. **32**, S221 (1961)] is a longstanding prediction – materials that become paramagnetic at a lower temperature along certain crystal directions while remaining magnetically ordered in other directions up to a higher temperature. Validating Callen's theory, we show that all directions within the basal plane of monoclinic $Fe_7S_8$ (pyrrhotite) single crystal remain ordered up to 603 K while the *c*-axis becomes paramagnetic at 225 K. Results prompt a re-evaluation of existing magnetic materials with a focus on magnetic characteristics along different crystal orientations *above* instead of below the ordering temperatures. Theoretical guidelines for identifying new materials with large anisotropy of Curie temperature are also given, and analysis protocol to characterize them in a self-consistent manner is discussed. Materials with such a large directional dependence of Curie temperature open the possibility for uniquely new devices and phenomena, including (spin) transport.

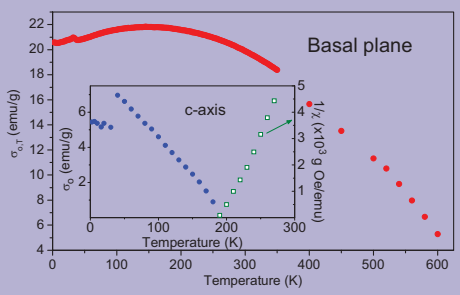


Anisotropic Curie temperature in pyrrhotite ($Fe_7S_8$). Notice the large difference in ordering temperature along basal plane (main graph) relative to the *c*-axis (inset).



**1 Introduction** Ferromagnetic and ferrimagnetic materials are characterized by a critical temperature below which magnetic interactions prevail over thermal agitation, leading to the appearance of a spontaneous magnetization. Above this critical point, called the Curie temperature, thermal energy eventually overcomes magnetic interactions and the material becomes paramagnetic.

It is less well known that the Curie temperature varies with the orientation of the crystal. In ordinary ferromagnets, this orientation dependence of Curie temperature is negligible because of the vanishingly small ratio of anisotropy to exchange energy, i.e., the spherical or isotropic exchange term dominates. Thus Curie temperature in ordinary ferromagnets *appears* to be an isotropic property, and assigning it a single characteristic ordering temperature suffices. However, a "small" difference is not equivalent to being the "same," and under appropriate set of conditions the anisotropy of Curie temperature is predicted to become appreciable, as discussed in the following.

In formulating the theory of "anisotropic magnetization" [1, 2], E.R. Callen and H.B. Callen [1] first discussed the "interesting possibility" of anisotropic Curie temperature or ACT; Callen and Callen noted that it was W. J. Carr, Jr. who initially raised this question, and they discussed it in detail at the Conference on Magnetism and Magnetic Materials (NY, November 1960), see footnote on page 320 of Ref. [1]. Soon thereafter, E.R. Callen [3, 4] developed the theory underlying the anisotropy of Curie temperature and conditions conducive to its observation.

**1.1 Anisotropy of magnetization and ACT** Closely related to magnetocrystalline anisotropy [5] is the

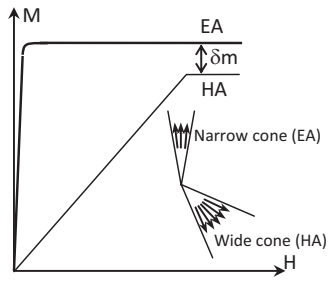


**Figure 1** Schematic illustrating the anisotropy of magnetization. Note that saturation magnetization is lower along the hard axis compared to the easy axis by an amount $\delta m$.

less well known anisotropy of magnetization [1, 2]. The latter's origins lie in magnetic anisotropy promoting the alignment of spins within a narrow cone along the easy axis while spreading them (a wider spin cone) along the hard direction. This leads to a smaller value of saturation magnetization along the hard axis compared to the easy axis, *cf.* schematic in Fig. 1. While this difference is negligible in ordinary ferromagnets (∼0.1% in Co) [1], it can become appreciable in materials with large magnetic anisotropy and/or small exchange energy. For example, in $YCo_5$ the effect is ∼4% at cryogenic temperatures [6].

Callen [3, 4] described the anisotropy of Curie temperature as follows: along the easy axis, the magnetic anisotropy tends to hold the spin cone and raises the Curie temperature, while along the hard axis anisotropy tends to spread the spin cone and lowers the Curie temperature. It is to be emphasized that perturbation theory is inadequate in formulating this effect. Using quantum mechanical internal field Hamiltonian, Callen [3, 4] showed that for large ratios of magnetocrystalline anisotropy energy to the exchange energy, *the moment along the hard axis drops abruptly to zero at a temperature that is lower than the Curie temperature along the easy axis*, i.e., ACT. In comparison, the anisotropy of Curie temperature is negligible in ordinary ferromagnets.

A promising candidate for ACT is the ferrimagnetic compound $Fe_7S_8$ (pyrrhotite; also called pyrrhotine), belonging to the Fe–S family; its investigation was also suggested by Callen [4]. The magnetic and crystal structure of the Fe–S family of compounds varies significantly with Fe/S ratio. Over time, this has given rise to significant confusion in the literature on results related to $Fe_7S_8$. Therefore, a brief survey of magnetic and crystal structure of $Fe_7S_8$ is given first prior to the description of experimental methods, results, and discussion.

**1.2 Crystal structure of $Fe_7S_8$** The crystal structure of $Fe_7S_8$ has been continually refined and verified using X-ray, neutron diffraction, and TEM [7–16]. At the request of Néel, Bertaut unraveled the true structure of $Fe_7S_8$ [9, 10] and found its diffraction spots to be inconsistent with the NiAs unit. Instead $Fe_7S_8$ has a pseudohexagonal structure that is slightly monoclinic with eight molecules of $Fe_7S_8$,

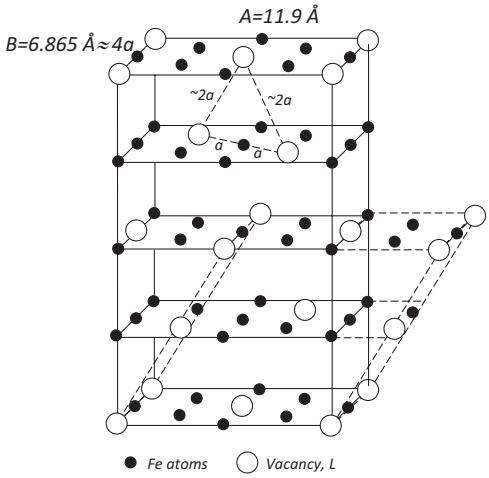


**Figure 2** Schematic structure of $Fe_7S_8$. Only iron planes containing ordered vacancies are shown. For clarity, iron planes without vacancies and intermediate sulfur planes are not shown. Following Bertaut [10].

see schematic in Fig. 2. Along the pseudohexagonal *c*-axis, the superstructure of $Fe_7S_8$ consists of iron planes separated by sulfur planes. With additional considerations of electrostatic exchange forces between iron atoms in iron-deficient $Fe_7S_8$, Néel concluded that this crystal is best represented as $Fe_7S_8L$, where L is a vacancy [17]. This gives rise to two sublattices for iron that are crystallographically different due to ordered vacancies in alternate iron layers normal to the *c*-axis. This asymmetry of iron sub-lattices also gives rise to ferrimagnetism and a magnetic symmetry within the basal plane that is lower than the crystal symmetry [13, 17].

**1.3 Magnetic structure of $Fe_7S_8$** Study of Pyrrhotite is closely intertwined with the beginnings of modern magnetism [5, 17–23]. Weiss [18] first reported magnetization curves along the basal plane of $Fe_7S_8$, with not enough results along the *c*-axis of $Fe_7S_8$. To extend Weiss' data, Pauthenet [24] measured magnetization along the *c*-axis and found a linear behavior in fields up to ∼20 kOe at room temperature. At lower temperatures, Pauthenet observed the appearance of a spontaneous magnetization along the *c*-axis. Néel described this "new phenomenon" as progressive superposition of a spontaneous magnetization on the "preceding paramagnetism" of the *c*-axis [17].

Magnetocrystalline anisotropy measurements show that the crystal exhibits a small triaxial symmetry within the basal plane [25], and the in-plane anisotropy constants have recently been refined [26]. In contrast, only a small linear increase in moment is observed along the *c*-axis even in fields as high as 100 kOe [27, 28]. This unusual behavior has been linked to ordered vacancies in alternate iron layers normal to *c*-axis [29]. A two-sublattice rotation molecular field model was also developed attempting to explain the linear behavior of $Fe_7S_8$ along the *c*-axis [30].

It is worthwhile noting that although Weiss [18, 20], Van Vleck [5], Néel [17], and others [24, 25, 30] referred to

 

the $c$-axis of $Fe_7S_8$ as being "paramagnetic" to describe its linear characteristics and to draw a contrast with the ferrimagnetic basal plane, their use of the term "paramagnetic" never implied a different Curie temperature along the $c$-axis relative to the basal plane of the crystal. It was Carr, Callen, and Callen who initially raised the possibility of ACT [1], and Callen [3, 4] who eventually developed the underlying theory of ACT.

**2 Experimental details and methods** Measurements were made on six different samples carved from two different natural crystals of $Fe_7S_8$. The chemical composition was confirmed using EDAX, which showed that the nominal composition of all the samples was close to $Fe_{0.875}S$ ($Fe_7S_8$), with composition varying slightly from $Fe_{6.86}S_8$ to $Fe_{7.26}S_8$ in different sections of the crystal.

The magnetization curves from 2 to 350 K were measured in a Quantum Design PPMS with a 70 kOe magnet. Another PPMS that was equipped with a 90 kOe magnet and high temperature VSM was used for measurements up to 640 K. The 70 kOe PPMS was also used to measure the ac susceptibility, with bias field up to 20 kOe, an ac field of 7 Oe, and excitation frequency from 10 Hz to 1 kHz. The magnetic moment and susceptibility was calibrated using a standard Pd sample. A room temperature VSM with a maximum field of ~8.8 kOe was used for preliminary analyses and screening of the crystals.

As our findings show, the $c$-axis of $Fe_7S_8$ becomes paramagnetic above ~225 K, and magnetization is confined within the basal plane above this temperature up to 603 K. Therefore, it is of critical importance to precisely align ($<1^\circ$) the magnetic field along the $c$-axis. This is non-trivial and must be stringently adhered to in experiments. We had to repeatedly perform an inordinate number of test runs to ensure precise alignments for each study. To prevent rotation at high fields, clamping is required; high temperature bending of the rod has to be avoided. If these precautions are not taken a parasitic moment from basal plane appears in the $c$-axis measurements. Examples of such spurious magnetization curves along the $c$-axis due to a misorientation of the $c$-axis relative to the applied field are shown in Ref. [27]; those authors estimated a misalignment of ~5–8°, which caused a spurious remanence to appear in what should otherwise be linear magnetization curves.

The specific heat $C_P$ of $Fe_7S_8$ was measured by heating the sample in a high resolution ac-calorimetry [31, 32] using a microfabricated chip, and these measurements were repeated 3 times in the temperature range of interest. Whereas the Curie peak at 603 K could easily be detected by a conventional DSC, it failed to resolve the peak from the noise at 225 K; hence the use of high resolution ac-calorimetry. As shown in Fig. 3, the ac calorimeter consisted of a thin film Pt heater and a sensor, both 100 nm thick, deposited on a 200 nm thick silicon nitride membrane supported by a silicon frame. The heater and sensor elements on the membrane were connected to gold leads on the silicon

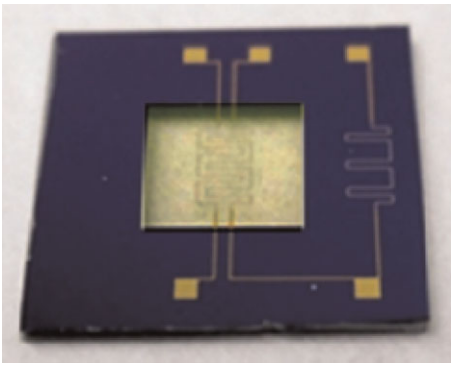

**Figure 3** (online color at: www.pss-b.com) Microfabricated ac-calorimetry chip for measurement of heat capacity.

frame. This design of ac calorimeter is similar to the one described in Ref. [33].

A Keithley 6221 ac current source was used for ac heating at a frequency of 2.25 Hz and amplitude of 0.4 mA. The resulting temperature oscillations were measured by passing a dc current (10 μA) through the sensor using another Keithley 6221 current source, and by measuring the corresponding voltage change using a lock-in amplifier (Stanford Research System SR830). The sample was fixed on the ac chip using N-grease (Apiezon). Prior to the measurements, the heat capacity of the chip with N grease was also measured to determine the heat addenda and also to rule out any extraneous peaks as a function of temperature. Measurements were made in the PPMS under vacuum (~$10^{-6}$ torr). Use of vacuum instead of high pressure He (~10 mtorr) in PPMS significantly reduces the drift and heat loss to the environment.

For the average transmitted power $P_o$ from the heater, the amplitude of temperature oscillations $T_{ac}$ is given by [31]:

$$T_{ac} = \frac{P_o}{\omega C}\left[1 + \frac{1}{(\omega\tau_1)^2} + (\omega\tau_2)^2 + \frac{2K_b}{2K_S}\right]^{-1/2} = \frac{P_o}{\omega C}F(\omega). \quad (1)$$

The time constant $\tau_1$ characterizes the chip-to-bath relaxation time. The time constant $\tau_2$ characterizes the response time of the sample and addenda (heater, thermocouple, and membrane platform) to a heat input, and $C$ is the total capacity of the sample and addenda. When $\omega\tau_1 \gg 1 \gg \omega\tau_2$, and the thermal conductivity of the sample $K_s$ is kept large with respect to sample-to-bath thermal conductivity $K_b$, then $F(\omega) = 1$, and Eq. (1) takes a simple form for the heat capacity of the sample $C_P \cong P_o/\omega T_{ac}$. In practice, the optimum operating frequency $\omega$ is determined by measuring the frequency dependence of $T_{ac}$ to obtain the "adiabatic plateau" by plotting $\omega T_{ac}$ versus frequency within the range of inequality [34]; the operating frequency $\omega$ is typically between $10^{-1}$ and $10^4$ Hz depending on the chip setup and sample [35]. A DSC calorimeter (Linkam

DSC 600) was used to determine the high temperature Curie transition at ∼603 K.

## 3 Results

**3.1 Basal plane characteristics** The fundamental property of interest in characterizing a magnetic phase at a given temperature is its spontaneous magnetization, $\sigma_{o,T}$ – the *magnetization within a single magnetic domain* of the crystal at zero-field. Practically, however, the measurement of $\sigma_{o,T}$ is complicated by the fact that magnetic materials generally exist as an aggregate of magnetic domains and direct measurement of $\sigma_{o,T}$ within a single domain is not feasible. While the application of magnetic field can erase the domains, the resulting quantity is *not* the spontaneous magnetization $\sigma_{o,T}$ but the specific magnetization at a given field $\sigma_{H,T}$. To overcome this problem, three principal methods have historically been developed (the so-called magnetic isotherm method, method of curves of constant magnetization, and measurements based on magneto-caloric effect) [36, 37]. The widely used magnetic isotherm method (employed in the present study) involves measurement of magnetization versus field, followed by extrapolation of the linear, high-field portion of the curve to zero-field [38]. Measurements are made at various temperatures, from which the temperature dependence of $\sigma_{o,T}$ can be determined. Also note that measurement of $M(T)$ or ZFC–FC does not yield the needed values of spontaneous magnetization, which is why we used the isotherm method.

Figure 4a–h show examples of magnetization curves at various temperatures with applied field along the basal plane; within the basal plane the direction of applied field was along the prism plane normal. Measurements were made by first heating the sample well above the overall Curie temperature of 603 K, followed by measurement of the magnetization curves at various temperatures. From Fig. 4, notice that the spontaneous magnetization doubles itself when the temperature is reduced from 540 to 150 K. Below ∼150 K, $\sigma_{o,T}$ begins to decrease. From such curves the temperature dependence of spontaneous magnetization $\sigma_{o,T}$ was determined, as shown in Fig. 5a.

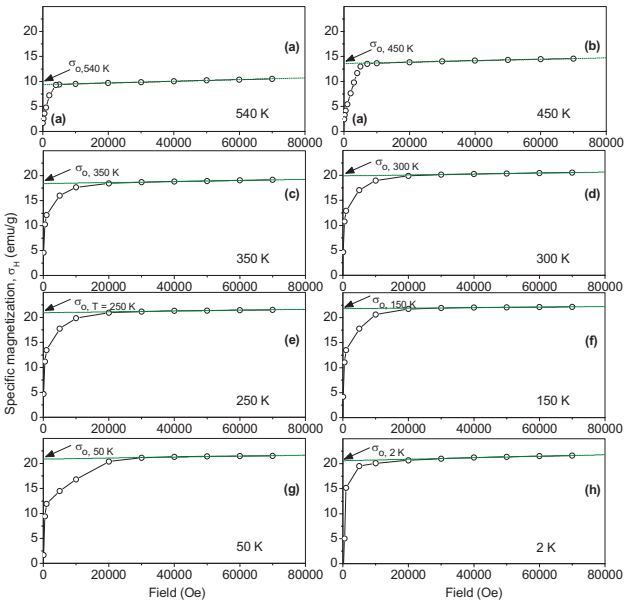


**Figure 4** Examples of in-plane magnetization curves at selected temperatures from which $\sigma_{o,T}$ is extracted. Extrapolation of $\sigma_{o,T}$ is done by the magnetic isotherm method.

The key point of Fig. 5a is that *the* basal plane remains spontaneously magnetized at all the temperatures up to 603 K.

Previously the Curie temperature of $Fe_7S_8$ has been determined by a variety of techniques, including susceptibility of the paramagnetic phase [11], calorimetry [12, 15], neutron diffraction [12, 16], and thermo-magnetic measurements [14, 16, 41]. Reported values range from 583 to 613 K, including those in synthetic crystals. See also Ref. [11] by Lotgering for an excellent discussion on the role of sulfur in the observed variation in Curie temperature. In one study (by Benoît), a Curie temperature of 565 K and an anomalous

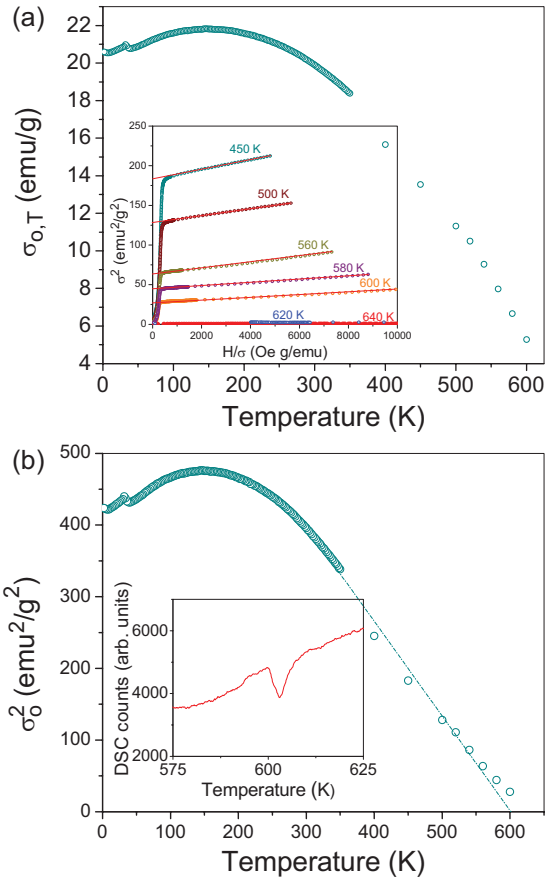


**Figure 5** (online color at: www.pss-b.com) (a) Temperature dependence of $\sigma_{o,T}$ as measured within the basal plane using isotherm plots such as the ones shown in Fig. 4. The transition at 34 K is characteristic of $Fe_7S_8$ composition [39, 40]. Inset shows Arrott plots using magnetization curves measured along the basal plane. (b) Extrapolation of Curie temperature from steepest portion of $\sigma^2_{o,T}$ versus $T$ curve. Inset: DSC trace on heating, showing Curie transition at ∼603 K.

susceptibility behavior above it was reported [42, 43], which was later referred to by Néel in discussing some of the characteristics of $Fe_7S_8$ [17]. However, Benoît's results in Ref. [42, 43] were subsequently shown by Lotgering to be a direct result of magnetite impurities ($Fe_3O_4$) in $Fe_7S_8$ [11].

We measured the Curie temperature of six samples from two different crystals by the technique of extrapolation of the steepest portion of the $\sigma^2_{o,T}$ versus $T$ curve [38, 44], see Fig. 5b, as well as by calorimetry, as shown in the inset of Fig. 5b. Data shows that the Curie temperature of the crystals is ~603 K, in agreement with previous studies. Arrott curves [45] are also plotted; see inset of Fig. 5a using the high temperature magnetization curves along the basal plane to further corroborate this value; it also confirmed the validity of using Arrott plots for analysis of this unusual material; Arrott plots are discussed in detail later in connection with determination of Curie temperature along the $c$-axis.

**3.2 Magnetic behavior along *c*-axis** Figure 6a–f show examples of magnetization curves along the $c$-axis at various temperatures. Higher temperature curves are characterized by linear magnetization curves, *cf.*, Fig. 6a. Although shown up to 70 kOe, this proportionality remained even in a 90 kOe magnet; it is known to persist even at higher fields [27, 28]. At low temperatures, a spontaneous magnetization gradually emerges and superimposes itself on the linear magnetization. The magnitude of this spontaneous magnetization increases as the temperature is lowered, and is accompanied by widening of the hysteresis loops, see Fig. 6. This "new phenomenon" was previously noted by Néel [17].

To investigate the appearance of spontaneous magnetization along the $c$-axis Arrott curves were plotted using the $c$-axis magnetization data. Note that Arrott curves are widely used to determine Curie temperature in ferro- or ferrimagnets by plotting $\sigma^2_{H,T}$ versus $H/\sigma_{H,T}$ isotherms [45], as shown in Fig. 7. In plotting these curves, care is taken to use fields that are sufficiently large to erase magnetic domains and hysteretic effects [46, 47]. At such fields that are sufficient to erase domains and hysteretic effects, the curves approach linear asymptotes, as shown by (red) lines in Fig. 7; also care has to be taken to avoid using too high fields in plotting the isotherms. The linear asymptote of the isotherm that passes

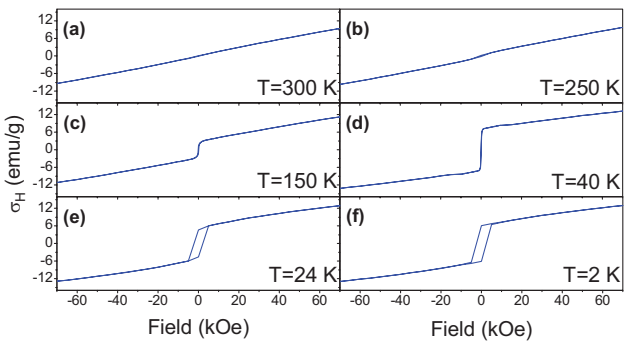


**Figure 6** (online color at: www.pss-b.com) Specific magnetization versus field at various temperatures along the $c$-axis of $Fe_7S_8$.

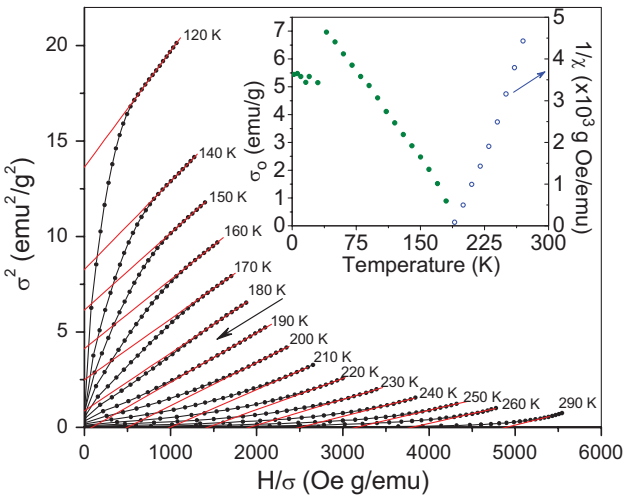


**Figure 7** (online color at: www.pss-b.com) Arrott curves ($\sigma^2_{H,T}$ vs. $H/\sigma_{H,T}$) along the $c$-axis at various temperatures. Inset shows $\sigma_o$ and $1/\chi$ versus temperature.

through the origin defines the Curie temperature. From Fig. 7, Arrott curves have a *positive* curvature above 190 K, and a *negative* curvature below 180 K, revealing a clear Curie transition from paramagnetism to ferrimagnetism. Extrapolation of linear asymptotes yields a Curie temperature of 186 K along the $c$-axis; Arrott plots along the basal plane showed a similar change in curvature at 603 K, see inset of Fig. 5a. In other words, the $c$-axis has a different Curie temperature than that along the basal plane.

For temperatures higher than the Curie point, the intercept along abscissa ($H/\sigma_{H,T}$) in Fig. 7 gives the inverse susceptibility $1/\chi$; at the Curie temperature, $1/\chi \to 0$ ($\chi \to \infty$). Below the Curie point, the intercept along the $y$-ordinate gives $\sigma^2_{o,T}$, from which spontaneous magnetization $\sigma_{o,T}$ can be determined. Temperature dependence of $1/\chi$ and $\sigma_{o,T}$ is shown in the inset of Fig. 7. Notice the drop in spontaneous magnetization close to the Curie temperature, as predicted by Callen [3, 4].

While Arrott curves clearly establish the existence of paramagnetic to ferrimagnetic transition along the $c$-axis, the exact value of Curie temperature is higher than 186 K because the isotherms are plotted as a function of applied field (as is the convention) without taking into account the demagnetization field. This along with other factors is well known to cause the Curie temperature to be underestimated by temperatures as much as 30 K [48, 49]. We did not include the effect of demagnetization factor. The demagnetization factor for the rectangular sample is ~0.144, and the demagnetization field, for example, at 150 K, is ~14 Oe. Demagnetization is one factor that can lead to an underestimation of Curie temperature, but it alone does not account for the entire shift. Other corrections are required that involve an arbitrary temperature dependent parameterization, see for example, Ref. [48–50]. Instead of making several assumptions regarding these corrections, the data for Arrott plots is left as measured. Instead of analytically

estimating the Curie temperature, it is possible and prudent to independently determine its precise value by direct measurement of other physical properties. This was done by measuring the temperature dependence of heat capacity $C_P$ using high sensitivity ac-calorimetery, Fig. 8a. The heat capacity shows a sharp lambda transition at 225 K; the inset in Fig. 8a shows a zoom-in view of $C_P$ in the vicinity of the Curie temperature. Due to increasing fluctuations in magnetic alignment, $C_P$ increases as the temperature is raised, and then drops abruptly at the Curie point. The observed lambda transition also matches with peaks in the derivative of ac susceptibility versus temperature, as shown in Fig. 8b; a similar anomaly at 225 K was also seen in dc susceptibility (not shown).

The lambda peak in Fig. 8a, which is <1.5 K wide, is too narrow to have been detected in the heat capacity measurements on $Fe_7S_8$ in Ref. [51], where data were taken every 10 K in this temperature range, and where the focus was on low temperature transition at 34 K. Also notice that

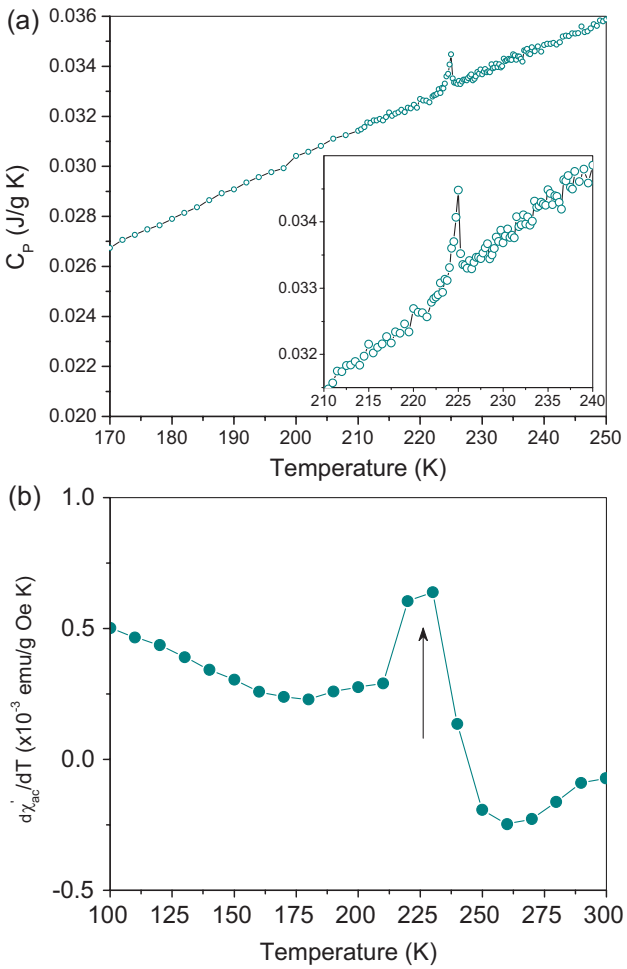


**Figure 8** (online color at: www.pss-b.com) (a) Temperature dependence of specific heat $C_P$ measured by ac-calorimetry. Inset shows a zoom-in view of the peak in the vicinity of the transition. (b) Derivative of ac susceptibility $\chi'$, measured at 20 kOe bias field, and 7 Oe, 1 kHz ac field.

while a sharp transition is evident in $C_P$, the anomaly in ac susceptibility is broader because the temperature interval for ac susceptibility ($\delta T = 10$ K) is 20 times larger than that for heat capacity ($\delta T = 0.5$ K). If measurements were taken at finer interval, the peak would indeed become sharper. Also, the measurements are made at an optimum bias field of 20 kOe. Too high bias fields cause contribution from basal plane to increase in the measured response.

With hindsight, it is of interest to note that a small blip can be seen in the neutron diffraction data in Ref. [16] close to 225 K but the authors never discussed the possibility of ACT, and instead speculated on a possible spin reorientation below 220 K. As discussed later, invoking spin reorientation transition is inadequate in explaining the entirety of the data presented here in a *self-consistent manner* (as discussed in detail in the following).

Moreover, the question is *not* about speculating the nature of magnetization *below* the transition; that would miss the entire point of Callen's concept. The question is: What are the magnetic characteristics of the *c*-axis *above* the transition temperature? To that question, our data clearly establishes that the *c*-axis exhibits paramagnetism and a distinct Curie temperature at 225 K, while at the same time the ferrimagnetic basal plane remains spontaneously magnetized at all temperatures up to 603 K. In other words, the material exhibits Callen's predicted anisotropy of Curie temperature along different crystal directions.

**4 Discussion** In conventional crystals, the Curie temperature is virtually independent of the crystal direction due to the miniscule ratio $\lambda$ of the anisotropy energy to the isotropic exchange energy ($\sim 10^{-5}$ for Fe and Ni, and $\sim 10^{-3}$–$10^{-4}$ in Co). The exchange energy for Fe and Co is $\sim 700\,\mathrm{cm}^{-1}$ and $10^3\,\mathrm{cm}^{-1}$, as compared to thermal energy $kT$ of $200\,\mathrm{cm}^{-1}$ at room temperature (expressed in terms of wave numbers for consistency of discussion by Callen and Callen, and Van Vleck) [1, 5]. For $Fe_7S_8$, an estimate for $\lambda$ can be made by plotting the measured value of spontaneous magnetization along the *c*-axis along with Callen's predicted values. Callen has shown that spontaneous magnetization $\langle S_\zeta \rangle$ as a function of temperature ($1/a$) can be expressed by the following *implicit* function [3, 4]:

$$\langle S_\zeta \rangle = \frac{e^{a\langle S_\zeta \rangle} - e^{-a\langle S_\zeta \rangle}}{e^{a\langle S_\zeta \rangle} + e^{-a\langle S_\zeta \rangle} + e^{a\lambda}}. \quad (2)$$

For $\lambda \leq 0.4621$, the Curie temperature is given by

$$a_C = 1 + \tfrac{1}{2} e^{\lambda a_C}. \quad (3)$$

Figure 9 plots magnetization along the *c*-axis for various values of $\lambda$ (solid lines). The reduced coordinates for temperature ($1/a$) from 0 to 1 scale with the ratio of thermal energy over exchange energy.

In Fig. 9, if $\lambda$ was negative, *c*-axis would be the easy axis, whereas positive values of $\lambda$ signify *c*-axis being the hard direction; the case of $\lambda$ equal to zero refers to an isotropic

 

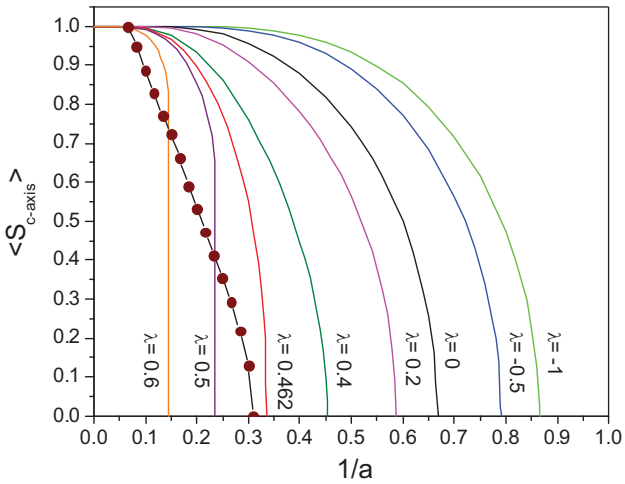


**Figure 9** (online color at: www.pss-b.com) Spontaneous magnetization $\langle S_{c\text{-axis}} \rangle$ versus temperature ($1/a$) using Eq. (2) (solid lines). The measured values are shown by solid symbols.

material. Equation (3) shows that for large negative values of $\lambda$, $a_c \to 1$. Therefore, $kT_c$ approaches the exchange energy; $k$ is the Boltzmann constant. As $\lambda \to 0$, $1/a_c \to 2/3$, i.e., $kT_c \to 2/3 \times$ exchange energy. As the value of $\lambda$ increases (becomes more positive), the anisotropy will cause the spin cone along the $c$-axis to spread and the magnetic order will disappear at a lower value of thermal energy, i.e., less $kT$ is needed to break the cone of magnetization, resulting in a lower Curie temperature along the $c$-axis. Using Eq. (2) and Fig. 9, the value at which spontaneous magnetization along $c$-axis drops to zero can be inferred, and $\lambda$ is found to be 0.467. Callen has shown that for $\lambda \geq 0.4621$, the magnetization is expected to drop discontinuously to zero, and this trend is apparent in the measured values.

Note that in the basal plane (easy plane) the sample can be saturated at relatively low fields. For example, at 150 K, saturation magnetization is 21.8 emu $g^{-1}$, see Fig. 5a. However, along the $c$-axis, even at 20 kOe the magnetization is just 5.6 emu $g^{-1}$, increasing to just 11.4 emu $g^{-1}$ at 70 kOe, see Fig. 6c. The field to achieve the saturation magnetization value (21.8 emu $g^{-1}$) as in the basal plane at this temperature can be estimated from extrapolation of the magnetization curve in Fig. 6c, until it reaches 21.8 emu $g^{-1}$, and it is ~150 kOe. This equates to a large anisotropy for the $c$-axis. This anisotropy has previously been estimated by Bin and Pauthenet, see Ref. [28], who arrived at anisotropy values on the order of 3–6 $\times 10^7$ erg $cm^{-3}$. Our own estimation puts a value ~2.5 $\times 10^7$ erg $cm^{-3}$.

It is also possible to arrive at the estimated anisotropy using the inferred value of $\lambda$ (= 0.467), which is the ratio of anisotropy to exchange energies. Along the $c$-axis with a Curie temperature of 225 K, taking density of $Fe_7S_8$ as 4.59 g $cm^{-3}$ and molecular weight of 648 g $mole^{-1}$, gives an anisotropy of 6.2 $\times 10^7$ erg $cm^{-3}$, which is comparable to the value obtained by Ref. [28].

As noted earlier, the fundamental quantity of interest in characterizing magnetism is the spontaneous magnetization. The data in Fig. 7 shows that with increase in temperature the spontaneous magnetization along the $c$-axis rapidly drops and vanishes below the room temperature, whereas Fig. 5 shows that the spontaneous magnetization within the basal plane remains finite up to 603 K. A casual inspection of hysteresis curves is insufficient to explain the observed behavior and it is for these very reasons that Arrott plots [45] and other techniques (the magnetic isotherm method, method of curves of constant magnetization, and measurements based on magneto-caloric effect [36, 37]) were historically developed to ascertain the magnitude of spontaneous magnetization. It is also of interest to note that the routine practice is to characterize the vanishing of the spontaneous magnetization (Curie point) by measuring its value along the easy axis. One rarely performs the challenging task of measuring it along the hard axis, the presumption being that Curie temperature is isotropic. However, as shown in Ref. [6] and schematically in Fig. 1, Callen and Callen's anisotropy of magnetization [1, 2] is a very demonstrable concept, and such measurements are needed (although rarely performed) to determine ACT. Therefore, attempting to describe the entirety of the data in terms of some spin reorientation transition leaves large inconsistencies in the interpretation of data; also use of the term "spin cone" is not exclusive to the description of the spin reorientation transition. In fact, it is suggested that one revisit some of the spin reorientation transitions and re-analyze them in terms of ACT.

Unlike conventional magnetic materials, the anisotropy of Curie temperature raises intriguing and interesting questions. For example, the role of magnetic domain structure within the basal plane in influencing the observation of the lower Curie temperature remains to be investigated. From the viewpoint of electron transport, Fig. 2 shows that $Fe_7S_8$ may be regarded as an ultimate magnetic multilayer with each monolayer of iron plane separated by a monolayer of a sulfur plane, and literature points to complex and interesting electron transport behavior [52–57]. Detailed measurements of magnetoresistance and magnetostriction are currently in progress and will be reported later.

Finally, theory guides that a large anisotropy raises the Curie temperature along the magnetic easy axes by holding the spins together, and causes it to spread the spins along the hard axes and lowers its Curie temperature. Therefore, high magnetocrystalline anisotropy and low exchange energy would tend to promote directional anisotropy of Curie temperature. It is also well known that lower the crystal symmetry, higher is the magnetocrystalline anisotropy. In the present context, candidate materials would have low crystal symmetry, large magnetocrystalline anisotropy, and/or weak exchange. Moreover, they would preferably be ferrimagnetic with magnetic symmetry that is lower than the crystal symmetry. Materials showing a large anisotropy of Curie temperature are also expected to exhibit anisotropy of compensation temperature in ferrimagnets.

As noted in the introduction, $RCo_5$ (R: rare-earth) intermetallics are known to have large magnetocrystalline anisotropy and a demonstrably large anisotropy of magnetization [6]. Similarly, Fe monolayers with large anisotropy and unusually large *g*-factor are candidates for further investigation [58]. In addition, over the past half century, anomalous behavior has also been observed in other isostructural crystals such as $Fe_7Se_8$, $Fe_7Te_8$, etc. [59–61]. Monoclinic iron phosphate is also of interest in this regard. Finally, magnetic materials with reduced dimensions are of special interest and exciting applications are anticipated in heterogeneous films (superlattices) where exchange can be engineered. ACT also raises interesting possibilities in terms of mobility of ferroelastic domains in high anisotropy magnetic shape memory alloys [62, 63], where low switching fields are desirable. In this regard, recent data on Heusler alloys coated inside hollow glass microwires [64] is suggestive of anisotropy of magnetization akin to that reported previously in Ref. [6] and Fig. 1, raising the possibility that such materials might also be candidates for exploring ACT.

**5 Conclusions** To conclude, we have experimentally realized Callen's prediction of anisotropic Curie temperature materials. Results prompt re-evaluation of existing materials with a focus on magnetic characteristics of crystal directions *above* instead of below the transition temperatures. Since all magnetic and transport properties are defined relative to the Curie temperature, results open the possibility for new devices and phenomena.

Instead of attempting to predict their usefulness, we conclude by recalling Kroemer's *Lemma of New Technology*: "The principal applications of any sufficiently new and innovative technology always have been – and will continue to be – applications *created* by that technology" [65].

**Acknowledgements** HDC and SZH gratefully acknowledge the sustained support and unrelenting encouragement of Shanta Chopra to pursue this work. This work was supported by the National Science Foundation, Grant Nos. DMR-0964830, DMR-0706074, and OISE-1157130, and this support is gratefully acknowledged. The ac-calorimetry chip was microfabricated at Cornell Nanofabrication Facility.

## References

[1] E. R. Callen and H. B. Callen, J. Phys. Chem. Solids **16**, 310 (1960).
[2] E. R. Callen, J. Appl. Phys. **31**, 149 (1960).
[3] E. R. Callen, J. Appl. Phys. **32**, S221 (1961).
[4] E. R. Callen, Phys. Rev. **124**, 1373 (1961).
[5] J. H. Van Vleck, Phys. Rev. **52**, 1178 (1937).
[6] J. M. Alameda, D. Givord, R. Lemaire, and Q. Lu, J. Appl. Phys. **52**, 2079 (1981).
[7] S. S. Sidhu and V. Hicks, Phys. Rev. **52**, 667 (1937).
[8] S. S. Sidhu and V. Hicks, Phys. Rev. **53**, 207 (1938).
[9] F. Bertaut, C. R. Hebd. Seances Acad. Sci. **17**, 1295 (1952).
[10] E. F. Bertaut, Acta Crystallogr. **6**, 557 (1953).
[11] F. K. Lotgering, Philips Res. Rep. **11**, 190 (1956).
[12] S. S. Sidhu, L. Heaton, and M. H. Mueller, J. Appl. Phys. **30**, 1323 (1959).
[13] M. Kawaminami and A. Okazaki, J. Phys. Soc. Jpn. **29**, 649 (1970).
[14] F. Li and H. F. Franzen, J. Solid State Chem. **126**, 108 (1996).
[15] F. Li, H. F. Franzen, and M. J. Kramer, J. Solid State Chem. **124**, 264 (1996).
[16] A. V. Powell, P. Vaqueiro, K. S. Knight, L. C. Chapon, and R. D. Sanchez, Phys. Rev. B **70**, 014415 (2004).
[17] L. Néel, Rev. Mod. Phys. **25**, 58 (1953).
[18] P. Weiss, J. Phys. Théorique Appl. **8**, 542 (1899).
[19] P. Weiss, J. Phys. Théorique Appl. **4**, 469 (1905).
[20] P. Weiss, C. R. Hebd. Seances Acad. Sci. **140**, 1587 (1905).
[21] P. Weiss, J. Phys. Théorique Appl. **4**, 829 (1905).
[22] P. Weiss and J. Kuntz, J. Phys. Théorique Appl. **4**, 847 (1905).
[23] J. H. Van Vleck, Rev. Mod. Phys. **17**, 27 (1945).
[24] R. Pauthenet, Comptes Rendus **234**, 2261 (1952).
[25] I. Mikami, T. Hirone, H. Watanabe, S. Maeda, K. Adachi, and M. Yamada, J. Phys. Soc. Jpn. **14**, 1568 (1959).
[26] F. Martin-Hernandez, M. J. Dekkers, I. M. A. Bominaar-Silkens, and J. C. Maan, Geophys. J. Int. **174**, 42 (2008).
[27] K. Sato, M. Yamada, and T. Hirone, J. Phys. Soc. Jpn. **19**, 1592 (1964).
[28] M. Bin and R. Pauthenet, J. Appl. Phys. **34**, 1161 (1963).
[29] K. Sato, J. Phys. Soc. Jpn. **21**, 733 (1966).
[30] M. J. Besnus, G. Munschy, and A. J. P. Meyer, J. Appl. Phys. **39**, 903 (1958).
[31] P. F. Sullivan and G. Seidel, Phys. Rev. **173**, 679 (1968).
[32] Y. A. Kraftmakher, Prikl. Mekh. Tekh. Fiz. **5**, 176 (1962).
[33] D. W. Denlinger, E. N. Abarra, K. Allen, P. W. Rooney, M. T. Messer, S. K. Watson, and F. Hellman, Rev. Sci. Instrum. **65**, 946 (1994).
[34] F. Fominaya, T. Fournier, P. Gandit, and J. Chaussy, Rev. Sci. Instrum. **68**, 4191 (1997).
[35] A. A. Minakov, S. B. Roy, Y. V. Bugoslavsky, and L. F. Cohen, Rev. Sci. Instrum. **76**, 043906 (2005).
[36] P. Weiss and R. Forrer, Ann. Phys. (Paris) **12**, 279 (1929).
[37] D. J. Oliver and W. Sucksmith, Proc. R. Soc. Lond. Ser. A, Math. Phys. Sci. **219**, 1 (1953).
[38] J. N. Armstrong, J. D. Felske, and H. D. Chopra, Phys. Rev. B **81**, 174405 (2010).
[39] P. Rochette, G. Fillion, J. L. Mattei, and M. J. Dekkers, Earth Planetary Sci. Lett. **98**, 319 (1990).
[40] G. Fillion and P. Rochette, J. Phys. Colloq. **49** (Suppl. 12), C8-907 (1988).
[41] M. J. Dekkers, Phys. Earth Planet. Inter. **57**, 266 (1989).
[42] R. Benoit, J. Chim. Phys. **52**, 119 (1955).
[43] R. Benoit, C. R. Acad. Sci. Paris **234**, 2174 (1952).
[44] J. Crangle and G. M. Goodman, Proc. R. Soc. Lond. A, Math. Phys. Sci. **321**, 477 (1971).
[45] A. Arrott, Phys. Rev. **108**, 1394 (1957).
[46] J. S. Kouvel, J. C. D. Graham, and J. J. Becker, J. Appl. Phys. **29**, 518 (1958).
[47] J. S. Kouvel and M. E. Fisher, Phys. Rev. **136**, A1626 (1964).
[48] É. D. T. d. Lacheisserie, D. Gignoux, and M. Schlenker (eds.), Magnetism: Fundamentals (Springer, New York, 2005).
[49] B. D. Cullity, Introduction to Magnetic Materials (Addison-Wesley Publ. Co., Reading, MA, 1972), p. 128.
[50] I. Yeung, R. M. Roshko, and G. Williams, Phys. Rev. B **34**, 3456 (1986).

 

[51] R. Grønvold, E. F. Westrum, Jr., and C. Chou, J. Chem. Phys. **30**, 528 (1959).
[52] E. Vitoratos and S. Sakkopoulos, J. Appl. Phys. **61**, 1928 (1987).
[53] C. Krontiras, K. Pomoni, and A. Theodossiou, J. Appl. Phys. **55**, 3894 (1984).
[54] K. Pomoni and A. Theodossiou, J. Appl. Phys. **53**, 8835 (1982).
[55] S. Sakkopoulos and A. Theodossiou, J. Appl. Phys. **45**, 5379 (1974).
[56] E. Hirahara and M. Murakami, Phys. Chem. Solids **7**, 281 (1958).
[57] K. Hirakawa, J. Phys. Soc. Jpn. **12**, 929 (1957).
[58] B. Chilian, A. A. Khajetoorians, S. Lounis, A. T. Costa, D. L. Mills, J. Wiebe, and R. Wiesendanger, Phys. Rev. B **84**, 212401 (2011).
[59] A. Kotani and N. Suzuki, Recent Advances in Magnetism of Transition Metal Compounds (World Scientific, Singapore, 1993).
[60] K. Shimada, T. Mizokawa, A. Fujimori, M. Shirai, and T. Kamimura, J. Electron Spectrosc. Relat. Phenom. **101–103**, 777 (1999).
[61] M. Shirai, N. Suzuki, and K. Motizuki, J. Electron Spectrosc. Relat. Phenom. **78**, 95 (1996).
[62] H. D. Chopra, C. Ji, and V. V. Kokorin, Phys. Rev. B **61**, R14913 (2000).
[63] M. R. Sullivan and H. D. Chopra, Phys. Rev. B **70**, 094427 (2004).
[64] V. Vega, L. Gonzalez, J. Garcia, W. O. Rosa, D. Serantes, V. M. Prida, G. Badini, R. Varga, J. J. Sunol, and B. Hernando, J. Appl. Phys. **112**, 033905 (2012).
[65] H. Kroemer, Rev. Mod. Phys. **73**, 783 (2001).